Rheological Properties of Styrene-*co*-2-Furfuryl Methacrylate Copolymers

Jose M. Rego,[1] Charles Berglund,[2] Gary Welsh,[2] Michael White[2]

[1]*Dow Benelux N. V., Plastics Research and Development, P.O. Box 48, 4530 AA Terneuzen, The Netherlands*
[2]*The Dow Chemical Company, Plastics Research and Development, Midland, Michigan 48674*

Received 24 May 2004; accepted 5 January 2005
DOI 10.1002/app.22240
Published online in Wiley InterScience (www.interscience.wiley.com).

ABSTRACT: The copolymerization of styrene with furfuryl methacrylate (FMA) led to a very significant molecular weight increase and to branching, as measured by standard gel permeation chromatography (GPC) and tri-angle laser light-scattering GPC. This increase was also confirmed by dynamic mechanical spectroscopy. Extensional viscosity analysis showed that styrene-*co*-2-furfuryl methacrylate copolymers exhibited strain hardening at low strain rates. This strain hardening is explained as a result of the copolymers' polydispersity features rather than a result of their topology. The presence of strain hardening in extensional viscosity experiments is believed to be advantageous in the production of foamed materials with lower densities. A reduction in density was corroborated by foaming experiments on a development extrusion line. The mechanism of density lowering was related more to cell growth than to increased nucleation. © 2005 Wiley Periodicals, Inc. J Appl Polym Sci 98: 1062–1071, 2005

Key words: branched; foams; molecular weight distribution/molar mass distribution; rheology

INTRODUCTION

Polystyrene (PS) is one of the major commercial polymers of the plastics portfolio. The main attributes of this polymer are its clarity and good processability. On the other hand, the main shortcoming associated with this material is its poor mechanical performance; specifically, it is highly brittle. Both brittleness and processability are the result of PS's high-entanglement molecular weight, which is generally accepted to be 18,000 g/mol.[1] The weight-average molecular weight (M_w) associated with commercial PS ranges from 150,000 to 325,000 g/mol. Higher molar masses (M_a's) are not economical due to the increase in conversion costs as M_w increases. It is apparent from this information that the triangle formed by the cost, processability, and brittleness is the main contradiction space that the PS industry faces, which makes it one of the industry's main research thrusts. Dow's research efforts to improve the balance within this triangle are numerous and include (1) anionic polymerization of styrene,[2–6] (2) branched PS,[7–11] (3) acid-mediated radical polymerization of styrene,[12–17] and (4) thermoreversible crosslinking of PS chains based on styrene-*co*-2-furfuryl methacrylate (SFMA) and bismaleimide[18,19] and other Diels–Alder chemistries.[20]

The production of SFMA copolymers to produce thermoreversible networks when reacted with bismaleimide has brought up interesting findings regarding the kinetic and rheological aspects associated with SFMA copolymers. Those discoveries led to a patent disclosure[21] on the benefits of these polymers for foam and oriented PS applications. Further details related to the copolymerization kinetics of these monomers were also published earlier.[22] The main observations related to these copolymers are that the addition of low concentrations of furfuryl methacrylate (FMA; see Fig. 1) increases the molecular weight of PS for a given polymerization rate and that the resulting polymers have different rheological properties than homopolymer PS made under the same conditions. In this article, we aim to provide the rheological data associated with this type of copolymer and to present a preliminary study of the foaming properties of these copolymers.

EXPERIMENTAL

Materials

FMA, styrene, ethylbenzene, and analytical tetrahydrofuran (THF) were purchased from Aldrich (Zwijndrecht, The Netherlands) and were used as received. The peroxide initiator 1,1-bis(*tert*-butylperoxy)cyclohexane (Trigonox™ 22) was purchased from Akzo Nobel (Arnhem, The Netherlands).

Production of the SFMA copolymers

The SFMA copolymers were produced in a PS miniplant setup composed of three reactors in series

Correspondence to: J. M. Rego (jmrego@dow.com).

Journal of Applied Polymer Science, Vol. 98, 1062–1071 (2005)

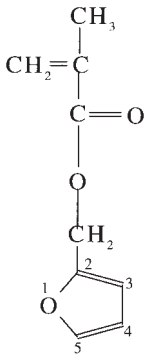

Figure 1 Molecular formula of FMA.

and a devolatilization–pelletizing unit. For simplicity, the SFMA samples were labeled by the nominal percentage of FMA in the copolymer (SFMA0, SFMA0.5, SFMA1.0, and SFMA1.6)

Analytical techniques

M_a moments were measured with a Hewlett-Packard HP9100 gel permeation chromatograph (Utrecht, The Netherlands) according to a Dow internal method and a calibration based on PS standards dissolved in THF.

True M_a's were measured with a tri-angle laser light-scattering gel permeation chromatography (TRALLS-GPC) instrument built in house (including a pump, auto sampler, column oven, and retractive index detector from Shimadzu (Hertogenbosch, The Netherlands); three polymer lab mixed B columns; and a Wyatt Minidawn detector). THF was also the solvent for this analysis.

Dynamic mechanical data were obtained in torsional shear with an ARES rheometer (Zellik, Belgium) with parallel plates 25 mm in diameter. Samples were compression-molded to a thickness of about 2 mm. Measurements were made at 200, 220, and 240°C at rates from 0.1 to 100 rad/s. Strains were kept in the linear regime.

Capillary data were obtained with a Goettfert 2003 triple-bore/triple-die rheometer (Buchen, Germany). Bagley and Rabinowitsch corrections were applied with standard Goettfert software. Samples were dried at 80°C for 2 h before testing. For low shear rate data, a Rheometrics DSR 500 controlled stress rheometer (Limonest Cedex, France) was used.

The extensional viscosity was measured on a Rheometrics RME Meissner-type extensional rheometer. Data were obtained at 160 and 170°C and at extensional rates of 0.01, 0.1, and 1.0 s^{-1}.

The low-density foam experiments were performed on a small-scale development line. Isobutane was the blowing agent used for all experiments. The blowing agent level was held constant at 4.5%, and the talc nucleator level was held constant at 0.66% for all experiments. A set of foam samples was produced over a range of melt temperatures, such that a density-versus-temperature relationship could be established for each resin at a given blowing agent level. Cell size was also measured for each set of samples. At each temperature, the die opening was adjusted to minimize prefoaming inside the die in an effort to produce the best possible foam quality.

TABLE II
Summary of the TRALLS-GPC Molar Mass Moments of the SFMA Copolymers

	M_w (amu)	M_n (amu)	M_z (amu)
SFMA0	303,000	146,000	491,000
SFMA0.5	360,000	148,600	686,000
SFMA1.0	435,000	155,000	990,000
SFMA1.6	490,000	165,000	1,270,000

RESULTS AND DISCUSSION

m_a moments

Gel permeation chromatography (GPC)

The PS standards–GPC M_a moments associated with the samples produced are given in Table I. The TRALLS-GPC M_a moments are given in Table II.

It is apparent from Tables I and II that (1) the M_a moments of SFMA0 were similar with both techniques, which indicated that this polymer backbone was linear; (2) the rest of the samples (which contained FMA) showed higher values of the M_a moments when measured by TRALLS-GPC than by PS standards–GPC. This difference was more marked at higher FMA

TABLE I
Summary of the PS Standards–GPC Molar Mass Moments of the SFMA Copolymers

	M_w (amu)	M_n (amu)	M_z (amu)	% > 2.5 MM	% > 1 MM
SFMA0	297,000	121,000	477,000	0	1.3
SFMA0.5	335,000	121,000	565,000	0	3.0
SFMA1.0	363,000	124,000	646,000	0	4.7
SFMA1.6	371,000	113,000	745,000	0.3	5.7

M_n, number-average molecular weight; M_z, z-average molecular weight; MM, million.

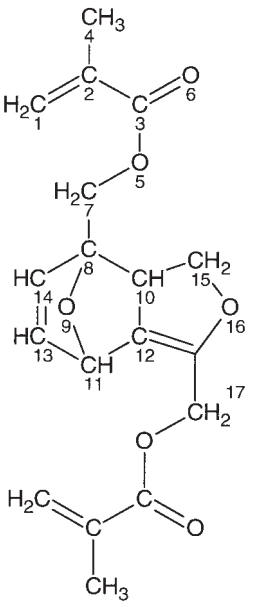

Figure 2 FMA dimer structure when the self-Diels–Alder reaction takes place between Furan groups.

contents (i.e., the difference was bigger for SFMA1.6 than for SFMA0.5); and (3) the polydispersity of the materials produced increased with increasing FMA content.

The differences in M_a as measured by TRALLS-GPC (true M_a) and PS standards–GPC (based on linear monodisperse PS standards) were generally attributed to branching. This confirmed other literature results that suggest that the furan ring is subject to radical reaction through its carbon 5 (C-5), which yields a stable allylic radical and a branched polymer.[23]

Dynamic mechanical spectroscopy

Another potential explanation for the difference in true and PS-calibrated GPC could be the addition of two furan groups through a Diels–Alder mechanism (see Fig. 2). This type of reaction is reversible with temperature. Accordingly, a decrease of M_a with an increase in temperature would prove that this reaction was taking place, assuming the measurements were made at temperatures where the depolymerization of PS was negligible (typically below 260°C). High-temperature GPC is not an accurate technique due to the poor signal-to-noise ratio for PS, which is attributed to the low values of concentration for PS in trichlorobenzene, but there is no other solvent that could be used for this purpose. Furthermore, the maximum temperature that can be attained with trichlorobenzene is 140°C.

Rheological measurements, however, can be used to determine the molar mass distribution (MMD) of a polymer at high temperatures in the melt. There are many approaches that can be used,[24–28] but they all require some type of rheological data over a broad frequency or time range, preferably 9 or more decades. The most common approach is to use dynamic mechanical data obtained at several temperatures to generate master curves with time–temperature superpositioning. Data covering 3 or 4 decades in frequency are obtained at each of several temperatures. Through the overlap of data from different temperatures, a master curve can be obtained that represents what the polymer's response would be over a very broad frequency range, as if the data had been obtained at a single temperature, the reference temperature. Methods based on the use of the storage modulus (G') and loss modulus or the complex viscosity (η^*) are used. For these approaches to work, it must be possible to generate a reliable master curve. Over the temperature range used to generate the data, the polymer must be thermorheologically simple, which means that the shapes of the rheological functions do not change with temperature, only the position on the log frequency axis. The shape of the master curve is primarily a function of the molecular weight distribution and branching, so if the FMA crosslinks were reversible, the SFMA copolymers would not be thermorheologically simple, and the master curves obtained from time–temperature superpositioning could not be used to determine molecular weight distributions. Another way of looking at the situation is that to determine the temperature dependence of the MMD (or branching), the MMD must be determined at specific temperatures and not from data at several temperatures. Because dynamic mechanical data can only be obtained over about 4 decades in frequency, it is not by itself adequate to accurately determine the MMD. At higher temperatures, data are more complete in the terminal zone (low frequencies), which accentuates high-M_a components, whereas at lower temperatures, the results are skewed toward low molecular weight. So the MMD calculated from data over a narrow frequency range may appear to change in shape as a function of temperature when it really does not. A possible remedy to this problem, and the one attempted here, is to combine the dynamic mechanical data at a particular temperature with creep (for low rate and long relaxation times) and capillary (high rate and short relaxation times) data at the same temperature to generate a true isothermal master curve.

The following procedure was applied in this study:[24–29] (1) η^* data were obtained from dynamic mechanical data at the desired temperature; (2) the Cox–Merz rule was applied to combine capillary (high rate) and η^* data; (3) low-shear-rate data obtained from creep experiments were combined with the η^* data; and (4) the Bueche model (which works well as the viscosity approaches the zero shear value) was used to fit the low- and medium-rate data, and the

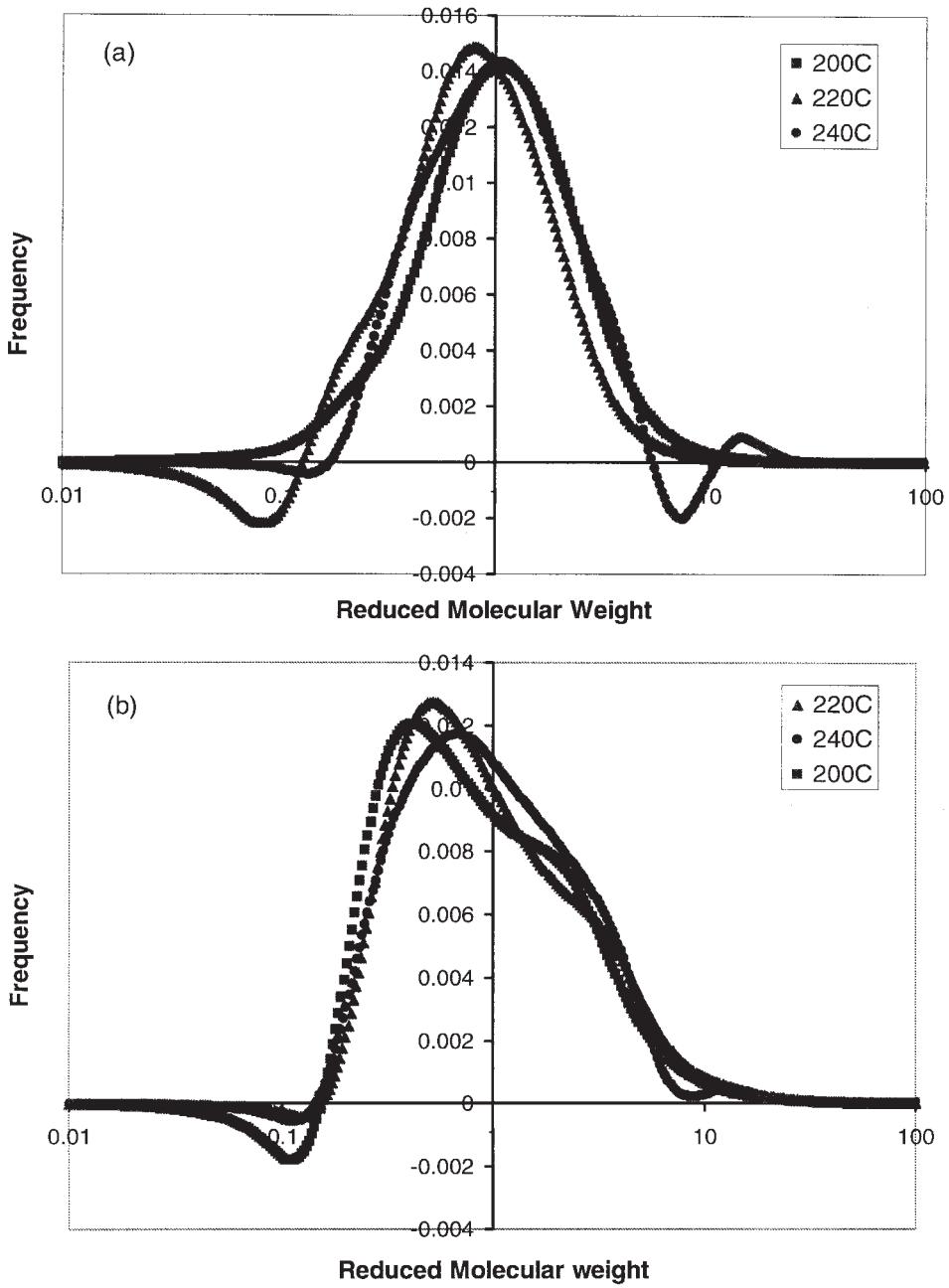

Figure 3 MMD at 200, 220, and 240°C, calculated from creep, dynamic mechanical, and capillary data for (a) SFMA0 and (b) SFMA1.6.

Vinogradow model (which fits the power law region well) was used to fit the high-rate data. Extrapolation was used if necessary to extend the time scales, and (5) the molecular weight distribution was calculated with eq. (3) from ref. 29 and eq. (9) from ref. 26.

Figure 3 shows the results of these calculations for SFMA0 [Fig. 3(a)] and SFMA1.6 [Fig. 3(b)], respectively. Each figure shows the results for each one of these materials at three different temperatures. Although the data indicate apparent shifts in MMD with temperature, the deviations below the baseline were obviously not real, and it was not clear whether the apparent shifts in MMD were real or an artifact of the computation technique. The calculated MMD for the SFMA1.6 copolymer shifted with temperature, but SFMA0, whose MMD should not have changed with temperature, also shows a shift with this procedure. These results cast doubt on the accuracy of the calculated MMD.

One possible origin of artifacts in the MMD calculation is irregularities or discontinuities in the master curve where the different types of data overlap. Liu et al.[25] illustrated the extreme sensitivity of the molecular weight distribution to subtle changes in the viscos-

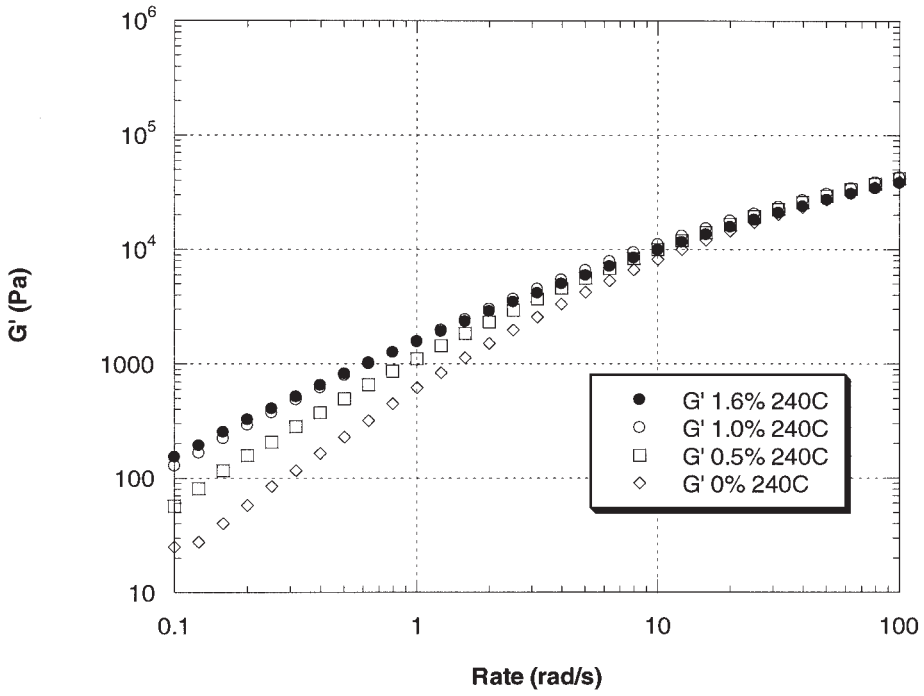

Figure 4 G' as a function of frequency at 240°C for all samples.

ity curve. Each knee in the viscosity curve can give rise to a peak or shoulder in the MMD, whether these knees are real or the result of imprecisely overlapping data. In this case, there are two possible problem areas. Capillary and dynamic data overlap at relatively high rates and tend to affect the low-molecular-weight part of the MMD. Creep and dynamic data overlap at lower rates and tend to influence the high M_a part of the MMD. To get an exact overlap in each of these areas would require that the Cox–Mertz rule be an exact relationship, which it is not.

G' data gave a qualitative view of how the FMA content affected M_a. Figure 4 shows G' as a function of frequency for all of the samples studied at 240°C. The increase in G' with increasing FMA content at low rates confirmed that the M_a moments increased with increasing FMA content. To further investigate the MMD changes, the calculation was repeated with only the dynamic mechanical data. The results obtained are shown in Figures 5(a) (for SFMA0) and 5(b) (for SFMA1.6). As shown in these figures, the baselines did not become negative, as they did for the curves shown in Figure 3. It would appear from Figure 5 that the MMD of SFMA0 was essentially independent of temperature, as it should have been. Data for this material also extended the farthest into the terminal zone at all temperatures. For SFMA1.6, which had even less complete data in the terminal zone, there was an indication of an apparent shift of the MMD to the high-molecular-weight end. The broadening of the MMD with FMA content was consistent with the qualitative assessment of G' and the GPC data.

On the basis of the analysis presented previously and an examination of the literature on the calculation of MWD from rheology data, it could be concluded that the asymmetry exhibited in Figure 3 was most likely an artifact of the calculation procedure and, in particular, a result of the combination of three types of data to obtain an isothermal master curve. Furthermore, the shifts in MMD observed in Figure 5 were too small to prove or disprove the hypothesis of a potential thermoreversible reaction between FMA groups. This would suggest that the M_a changes must have been associated with the introduction of branching through C-5, as indicated earlier.

Extensional viscosity

Figure 6 shows the change of extensional viscosity with time for all samples studied at 160°C and for strain rates of 0.01 s^{-1} [Fig. 6(a)] and 0.1 s^{-1} [Fig. 6(b)]. At a strain rate of 0.01 s^{-1}, the FMA containing polymers had significantly higher extensions than SFMA0. This difference in behavior may have been due to the higher M_a of the FMA-containing polymers or to the introduction of branching. At the higher rates, there was no systematic difference between the materials containing different amounts of FMA. Some strain hardening was observed, but the degree of strain hardening did not depend on the amount of FMA.

To further investigate the potential impact of branching on the rheology of these SFMA copolymers, we tried to model the extensional viscosity with the

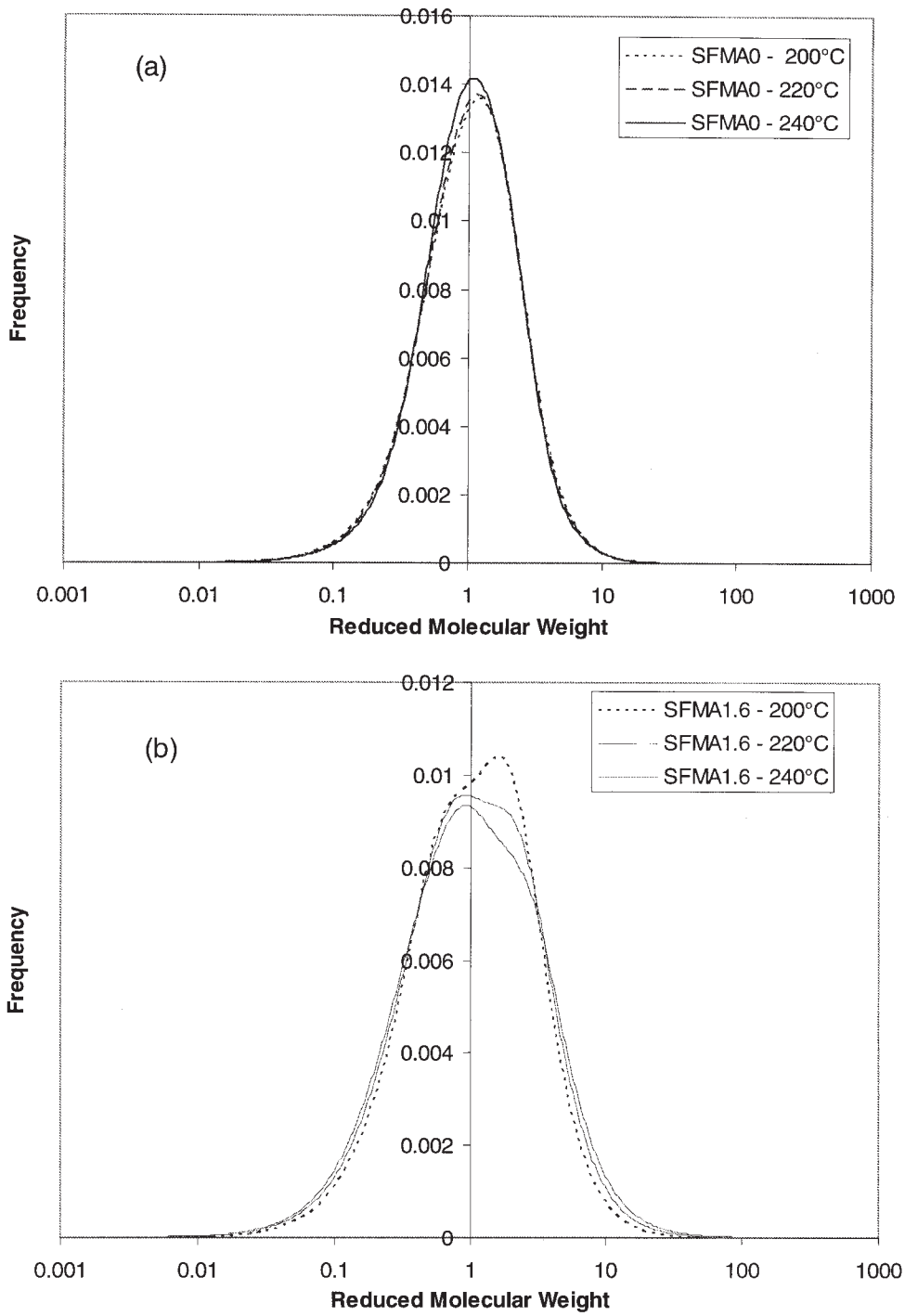

Figure 5 MMD at 200, 220, and 240°C, calculated from dynamic mechanical spectroscopy capillary data for (a) SFMA0 and (b) SFMA1.6.

pom-pom model. The pom-pom model (based on the tube, or reptation, model of polymer relaxation) has been successfully applied to relate the rheological behavior of highly branched polyethylene to its branching structure.[30,31]

In its simplest manifestation, as illustrated in Figure 7, a pom-pom molecule is composed of a linear backbone (the crossbar) with a molecular mass (M_b) several times the entanglement M_a, and branch points at each end. These branch points have functionality (q + 1) and M_a, and the number of branches (q) must have a value of 2 or more to constitute a pom-pom. As long as M_b and M_a are both several times larger than the entanglement M_a, pom-pom molecules will exhibit more strain hardening in extension than linear molecules with the same total M_a.

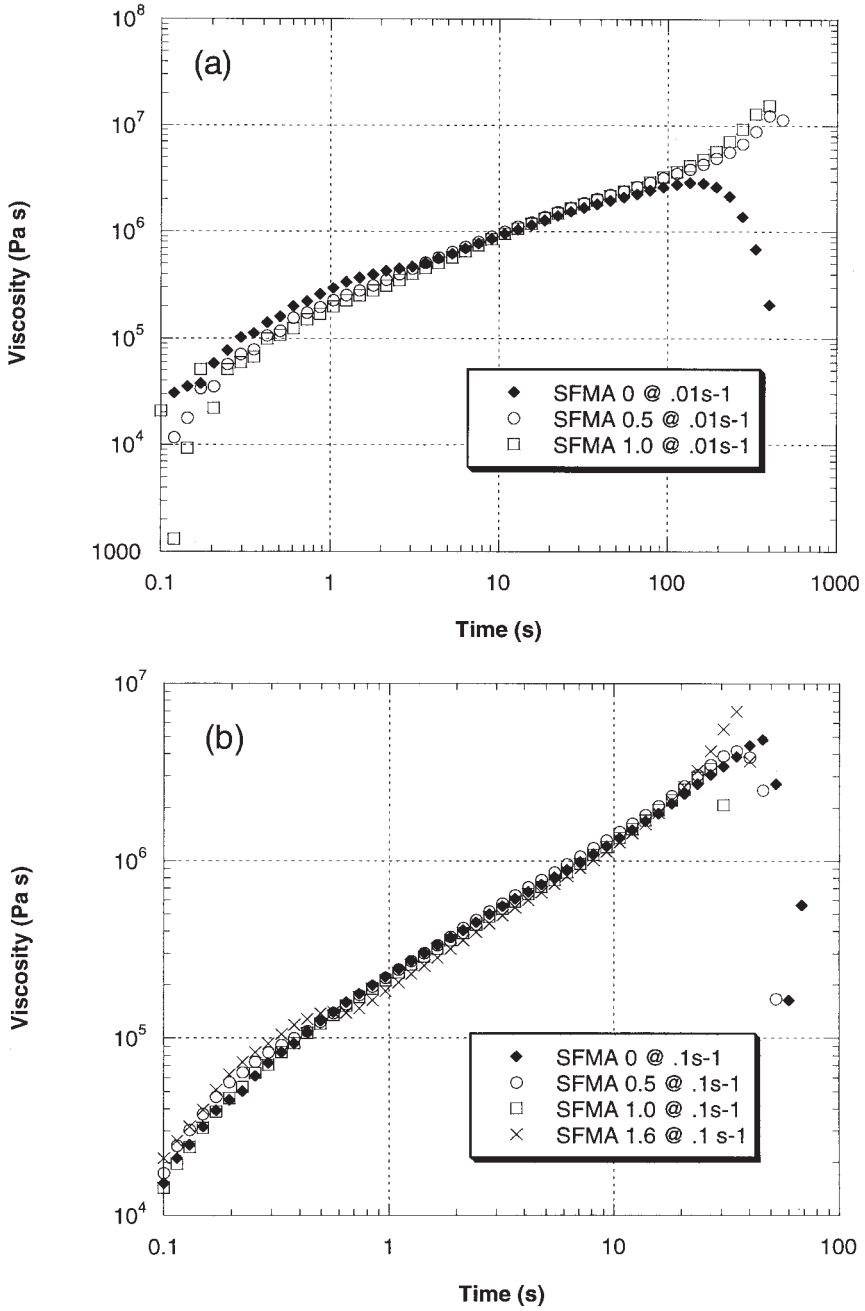

Figure 6 Extensional viscosity at 160°C and for strain rates (a) 0.01 and (b) 0.1 s^{-1}.

The fundamental reason for this strain hardening is the suppression of the relaxation of the branch points. For a simple pom-pom with two branch points, the degree of extension hardening increases as q increases.[30] For more complex (real) molecules with multiple branch points, q can have small values ($\sim$3) for branch points at the extremities of the molecule and much larger values for branch points near the center. The parameter q is determined from the total number of branches emanating from a point, so for a multiply branched molecule (e.g., a dendrimer), q can have values much larger than the branch-point functionality.

In practice, the pom-pom model is applied by the assumption of a set of discrete relaxation times and the fitting of the model to transient extensional data to determine a modulus and value of q corresponding to each relaxation time. Shear data are not sensitive to branching. For low-density polyethylene, which is well known to be highly branched, the pom-pom model calculates values of q as high as 150 for the longest relaxation times and smaller values of q for shorter relaxation times, which arise from branch points farther from the center of the molecule.

Figure 8 shows an example of the transient extensional data for SFMA0 at 170°C and a strain rate of 0.1

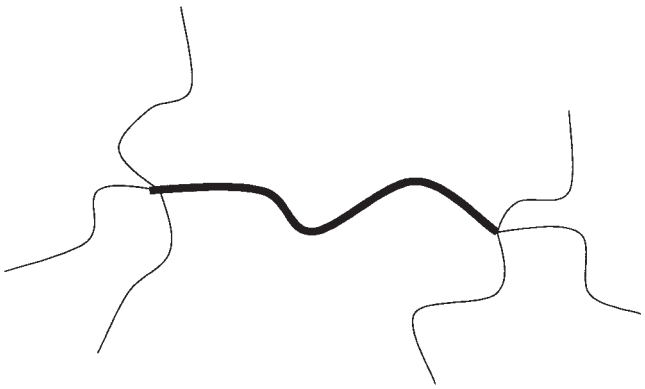

Figure 7 Schematic of pom-pom with two branch points and $q = 3$. The heavy line represents the crossbar.

TABLE III
Pom-Pom Model Parameters for SFMA0

Relaxation time (s)	Modulus (Pa)	q
0.0360	20,318	1
0.1296	24,300	1
0.4660	28,354	1
1.6750	27,096	1
6.0197	18,553	10
23.633	9,821	1
82.747	3,184	1
298.41	460	1
1071.15	60	1
3861.73	8	1

s^{-1} (lower curve) and at 160°C and a strain rate of 1.0 s^{-1} (upper curve). The symbols represent the experimental data, and the solid lines represent the fit of the pom-pom model with 10 relaxation times. The parameters extracted from the fit are listed in Table III.

The expected results for SFMA0, which was a linear molecule, were that all q values should have been 1. The model can only attribute strain hardening, whether real or not, to branching. In this case, there was some apparent strain hardening, which may have been only a polydispersity effect, and that was reflected in a q value of 10 for an intermediate relaxation time. This result was not physically realistic.

The results for SFMA1.6 are given in Table IV. The experimental data showed strain hardening, which resulted in relatively large values of q. However, q was largest for intermediate values of the relaxation time, not the longest, and this result was not physically realistic. Most likely, the strain hardening was a result of polydispersity (a high-molecular-weight component) and was not due to long-chain branching as in the case of low-density polyethylene.

The reason the pom-pom model failed for SFMA1.6 could have been that there was not sufficient branch-

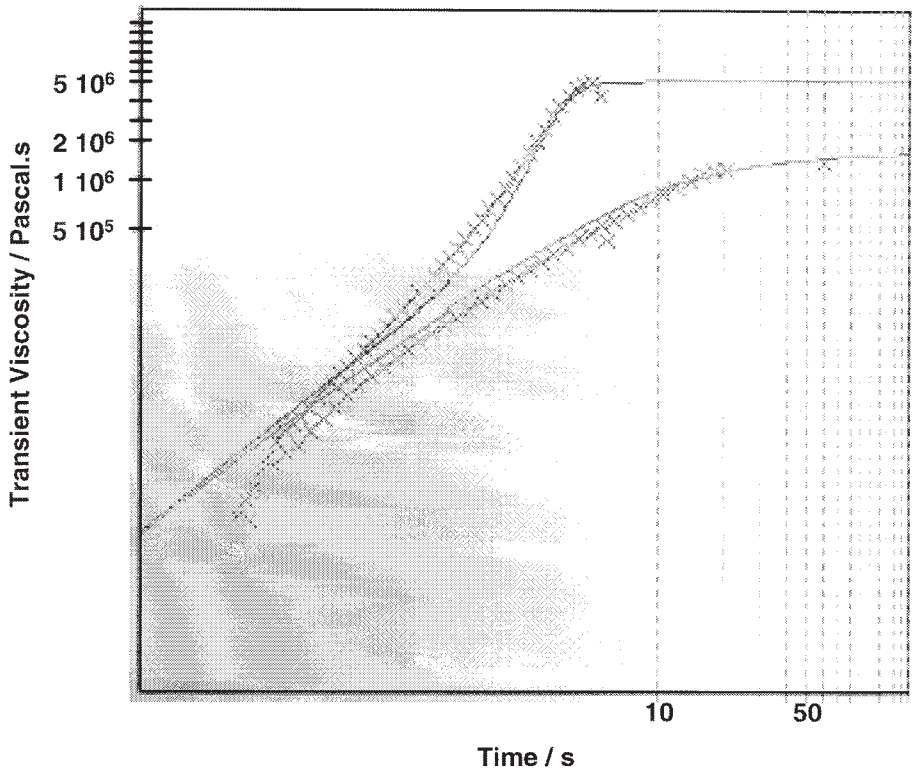

Figure 8 Transient extensional data and pom-pom model fit for SFMA0 at (lower curve) 170°C and 0.1 s^{-1} and (upper curve) 160°C and 1.0 s^{-1}. The symbols are the experimental data, and the solid lines are the best fit.

ing to result in a true pom-pom molecule. An assumption made in the derivation of the model[30,31] is that the bar relaxation time is much longer than that of the arms. This condition was difficult to realize in SFMA copolymers for two reasons. First, the concentration of FMA was not sufficient to introduce several well-spaced (at least several entanglement M_a's) branch points into the molecule. Second, the entanglement M_a of PS was so large (18,000) that it was much more difficult to have crossbars and arms with molecular weights several times larger, unlike the case for polyethylene. It could be concluded, therefore, that the strain hardening observed with the SFMA polymers was a result of their larger polydispersity (viz., the presence of the high-molecular-weight component) and not to long-chain branching as in the case of low-density polyethylene.

Foaming results

The foaming results are summarized in Table V. The results in Table III indicate that lower densities were obtained with increasing FMA concentration. Furthermore, the foaming window shifted toward higher temperatures. Note also that the cell size became larger with additional FMA concentration. It would appear from the results given that the mechanism for the foaming behavior observed with increasing levels of FMA was increased cell growth rather than increased nucleation. The reason for this behavior could have been related to the extensional rheological behavior of the SFMA copolymers. The additional extensional melt strength allowed this extra cell growth to occur without collapsing the cells.

Although it appears that SFMA1.6 could be foamed to lower densities at higher temperatures, it did appear to have a narrower processing window as well. Above a die melt temperature of 158°C, the foam tended to collapse very quickly. On the low end of the temperature range explored for this sample, the polymer gel started to freeze off inside the extrusion equipment. Between the high and low temperatures, we had to manage the die gap very carefully to allow foaming to take place without freezing the polymer off inside the extruder (pressure too high) and without the polymer gel foaming inside the die (pressure too low). SFMA1.0 behaved in this manner as well but to a lesser extent. In contrast, SFMA0 and SFMA0.5 required little adjustment to the die to produce acceptable foam.

TABLE IV
Pom-Pom Model Parameters for SFMA1.6

Relaxation time (s)	Modulus (Pa)	q
0.0385	28,056	1
0.1384	26,662	1
0.4974	24,753	1
1.7876	19,728	5
6.4243	12,100	33
23.087	6,127	20
82.973	2,611	13
298.19	958	4
1071.6	335	1
3861.2	116	1

TABLE V
Foaming Experiment Results

Resin	Die melt T (°C)	Outlet die P (psi)	Density (lb/f1^3)	Cell size (μm)
SFMA0	154	751	3.42	290
	149	935	3.2	220
	147	994	2.93	180
	144	1008	3	180
	143	972	3.17	210
SFMA0.5	159	718	3.47	310
	157	759	3.3	280
	155	752	3.23	320
	150	919	3	250
	146	916	2.9	280
SFMA1.0	159	752	3.85	320
	155	769	3.2	310
	153	829	3.09	250
	151	867	2.8	230
	147	964	2.89	270
SFMA1.6	158	804	3.64	320
	155	870	3.15	320
	152	935	2.8	280
	150	938	2.3	310
	149	1086	2.8	290

CONCLUSIONS

The copolymerization of styrene with FMA led to a very significant molecular weight increase and to branching. This result was confirmed by GPC, TRALLS-GPC, and dynamic mechanical spectroscopy. Extensional viscosity analysis showed that the SFMA copolymers exhibited strain hardening at low strain rates. This strain hardening was explained as a result of the copolymers' polydispersity features rather than their topology.

The presence of strain hardening in extensional viscosity experiments is believed to be advantageous for the production of foamed materials with lower densities. This was corroborated by foaming experiments on a development extrusion line. The mechanism of density lowering was related more to enhanced cell growth than to increased nucleation.

The authors thank Dr. Nathaniel Inkson for modeling the elongational viscosity behavior of the SFMA copolymers with the pom-pom model.

References

1. Graessley, W. W. Adv Polym Sci 1974, 16, 14.
2. Priddy, D. B.; Pirc, M. U.S. Pat. 84-633834 (1986).
3. Priddy, D. B.; Pirc, M. Polym Prepr 1988, 29, 340.
4. Priddy, D. B.; Pirc, M. J Appl Polym Sci 1989, 37, 393.
5. Priddy, D. B.; Pirc, M. J. Appl Polym Sci 1989, 37, 1079.
6. Priddy, D.; Pirc, M.; Meister, B. Polym React Eng 1993, 1, 343.
7. Tinetti, S. M.; Priddy, D. B. U.S. Pat. 95-386568 (1995).
8. Tinetti, S. M.; Faulkner, B. J.; Nelson, R. M.; Priddy, D. B. Presented at the 212th American Chemical Society meeting, Orlando, FL, August 1996.
9. Tinetti, S. M.; Faulkner, B. J.; Nelson, R. M.; Priddy, D. B. Polym Prepr 1996, 37, 540.
10. Pike, W.; Priddy, D. B.; Vollenberg, P. H. T. WO Pat. 96-US15954 (1997).
11. Priddy, D. B. WO Pat. 97-US11265 (1998).
12. Buzanowski, W. C.; Graham, J. D.; Priddy, D. B.; Shero, E. Polymer 1992, 33, 3055.
13. Priddy, D. B.; Dais, V. A. WO Pat. 95-US14191 (1996).
14. Pike, W.; Priddy, D. B. WO Pat. 98-US8392 (1999).
15. Roe, J. M.; Rego, J. M.; Priddy, D. B. U.S. Pat. 6084044 (2000).
16. Pike, W.; Priddy, D. B.; Roe, J. M.; Rego, J. M. WO Pat. 2000-US9945 (2000).
17. Matthews, B. R.; Pike, W.; Rego, J. M.; Kuch, P. D.; Priddy, D. B. J Appl Polym Sci 2003, 87, 869.
18. Goiti, E.; Huglin, M. B.; Rego, J. M. Eur Polym J 2004, 40, 219.
19. Goiti, E.; Huglin, M. B.; Rego, J. M. Macromol Rapid Commun 2003, 24, 692.
20. Goiti, E.; Huglin, M. B.; Boag, N. M.; Rego, J. M. Surf Coat Int Part B: Coat Transact 2002, 85, 235.
21. Rego, J. M.; Aerts, L. M.; Priddy, D. B.; Demirors, M. WO Pat. 2001-US23385 (2002).
22. Goiti, E.; Huglin, M. B.; Rego, J. M. Polymer 2001, 42, 10187.
23. Davidenko, N.; Zaldivar, D.; Penishe, C.; Sastre, R.; San Roman, J. J Polym Sci Part A: Polym Chem 1996, 34, 2759.
24. Tuminello, W. H. Polym Eng Sci 1986, 26, 1339.
25. Liu, Y.; Shaw, M. T.; Tuminello, W. H. Polym Eng Sci 1998, 38, 169.
26. Shaw, M. T.; Tuminello, W. H. Polym Eng Sci 1994, 34, 159.
27. Giudici, R.; Scuracchio, C.; Bretas, R. E. S. J Appl Polym Sci 2000, 75, 1416.
28. Llorens, J.; Rude, E.; Marcos, R. M. J Polym Sci Part B: Polym Phys 2000, 38, 1539.
29. Wood-Adams, P. M.; Dealy, J. M. J Rheol 1996, 40, 761.
30. McLeish, T. C. B.; Larson, R. G. J Rheol 1998, 42, 81.
31. Inkson, N. J.; McLeish, T. C. B.; Harlen, O. G.; Groves, D. J. J Rheol 1999, 43, 873.